Budapesti Műszaki és Gazdaságtudományi Egyetem
Pál Vásárhelyi Doctoral School of Civil Engineering and Earth Sciences

Determination of Traffic Load Induced Accumulating Permanent Strains of Granular Soils under Flexible Pavement Structures

Ph.D. Thesis new scientific results

Máté János Vámos
Civil Engineer

Suervisor:

PhD. Szendefy János

Associate Professor

Mannheim, 2024

TABLE OF CONTENTS

1 INTRODUCTION

The goal when designing a pavement is to find the most economical combination of pavement material and thickness by also considering the local climatic and ground conditions in such a way that the pavement is capable of bearing the traffic over its design lifetime without restricting its functionality. Failure of the pavement or restriction of its functionality can be caused by fatigue cracking or excessive rutting. It is crucial to reduce rutting in order to offer long service life and safe pavement structures, since besides of the serviceability rutting is considered as a major safety issue for vehicles. In international literature, rutting caused by loading can originate from asphalt due to insufficient compaction or improper asphalt mix composition, or it can be soil-related, resulting from cumulative permanent deformations in the soil under repeated loading. In domestic literature, rutting refers to deformations occurring within the asphalt layers only, while soil-related compressions are termed pavement subsidence. My research focuses on soil-related pavement deformations and settlements; the undesirable compression of asphalt layers is not considered in the calculations.

1.1 Topicality

In the case of geotechnical structures, meeting the serviceability limit state is often more challenging than satisfying the load-bearing requirements. For reliable, efficient, and economical operation, it is essential to accurately estimate the deformations of the structures, understand the subsoil's response to repeated or dynamic impacts, and gain as precise an understanding as possible of the influencing factors.

The impact of road transportation on the economy and society is undeniable. In Hungary in 2023, nearly 70% of freight transport and almost half of intercity public passenger transport were conducted by road (KSH, 2024). Despite this, excluding highways, 44% of the national road network was still rated as poor (category 5) in terms of pavement condition in 2023, with an additional 9% classified as inadequate (category 4). The roughness

grades assess the roads' waviness and rutting. From this perspective, the road network presents a somewhat more favorable picture than in terms of surface integrity. A total of 15,000 kilometers, or half of the national network excluding highways, was rated as good or adequate, while 32% (10,000 kilometers) fell into the poor or inadequate categories. The length of particularly dangerous sections with ruts 17 mm or deeper, which pose a significant accident risk, was nearly 1,200 kilometers in 2023, accounting for 4% of the entire network managed by Magyar Közút (Magyar Közút, 2024).

The research field of soil compression beneath flexible pavement structures is a neglected area, as the current practice of road pavement design does not thoroughly address this issue. In domestic practice, the prevailing attitude is that if the prescribed quality and construction standards are adhered to during implementation, the vertical compression of the subgrade is not expected to pose a critical load for the lifespan of the pavement structure. The relevance of the topic is further emphasized by the ongoing global climate change, which necessitates replacing previously well-functioning empirical correlations with scientifically grounded models that help understand the impact of changed boundary conditions on the built environment.

When we look at international road engineering standards, even one of the most modern, the RDO (RDO - Asphalt 09, 2009), addresses rutting in a relatively simple manner. If the prescribed allowable vertical stress at the top of the subgrade is maintained, significant damage due to rutting is not anticipated. However, the RDO does not quantify rut depth, and we cannot determine deterioration over the pavement's lifespan (Zeißler, 2021). Similar to the German standard, the Belgian CRR research institute (Verstraeten et al., 1982) examines the tendency for rutting by limiting deformation at the top of the subgrade, but it also does not quantify it. The mechanical-empirical design method developed by domestic researchers (Tóth and Primusz, 2020)also uses the CRR institute's formula to assess rutting. The Australian standard (Austroads, 2019) specifies the allowable number of standard axle (8 t) passes without excessive rutting, which has been proven effective in practice under Australian environmental conditions according to the design guide.

The literature is also not consistent regarding the origin of ruts. According to a recent review (Albayati, 2023), ruts form exclusively in the asphalt layer, with the underlying granular layers not contributing to permanent deformations. Consequently, several recent studies have focused on describing the rheological properties of asphalt (Gajári, 2019; Gajári et al., 2021) and emphasizing the resistance of asphalt mixtures to rutting (Aljbouri and Albayati, 2023; Bharath et al., 2023; Toth et al., 2024; Zhang et al., 2023). In contrast, field studies conducted by AASHTO revealed that 68% of permanent deformations occur not in the asphalt but in the underlying base and subbase layers, as well as in the subgrade (Morris, 1973)). A more recent study (White et al., 2002)published similar findings. Based on these results, when examining rutting in pavement structures, research and computational methods should focus more on the soils rather than the asphalt.

1.2 Aim of the research

According to a recent literature review (Singh and Sahoo, 2021), there is currently no widely recognized, validated, and practical computational method that adequately describes the long-term behavior of soils under pavements when subjected to cyclic loading. Certain methods (Werkmeister, 2003) focus exclusively on the base and subbase layers, thus neglecting the influence of the subgrade. Other studies (Uzan, 2004) appear very promising, but the calibration of material constants is not described, making them unusable under different boundary conditions. Some research (Qi et al., 2022; Zhou et al., 2022) determines the permanent deformations of soils beneath pavement structures using a creep-like material model and 3D finite element analysis. However, the material model was calibrated using only 1,000 cycles of triaxial testing, which raises doubts about its validity for pavement structures, where it is often necessary to examine several (tens of) millions of axle passe

The objectives of my doctoral research were as follows:

- Develop a universal calculation method that operates effectively under varying boundary conditions to determine the accumulating permanent deformations in granular soils beneath flexible pavement structures due to repeated traffic loading.
- Describe the spatial and temporal progression of the resulting deformations and settlements.
- Determine the stress and deformation conditions prevailing in the soil layers due to preloading during construction.
- Investigate the impact of different granular subgrade types and traffic load classes on the resulting deformations and settlements.

- Clarify the extent to which each structural layer (base, subbase, subgrade) contributes to the total pavement settlement.
- Examine the effects of changes in other boundary conditions, such as temperature, axle load, subbase layer thickness and material, on the resulting settlements.
- Compare the expected pavement settlements of typical domestic pavement structures with those of similar empirically-based pavement structures from other nations.

Since my research field lies at the intersection of multiple disciplines—specifically road engineering, geotechnics, and mechanical material modeling—my goal with this dissertation is to spark further discussion among experts and researchers from these fields, fostering a better mutual understanding of each other's work

2 METHODOLOGY

2.1 HCA-model

In the case of high-cycle loading, implicit methods that directly calculate deformations are not effective because with each loading cycle, we accumulate and carry forward material model and computational (integration) errors. As a result, these methods can only be reliably used for up to about N < 50 cycles (Niemunis, 2003). Therefore, explicit solution methods are preferred, which empirically determine the relationship between the number of cycles and residual deformation ($\mathrm{N} - \varepsilon^{acc}$). One of the most well-documented material models of this type, verified by numerous laboratory tests for determining residual deformations resulting from repeated loading, is the High-Cycle Accumulation (HCA) model, published by (Niemunis et al., 2005) and validated through various model experiments in Wichtmann's doctoral dissertation (Wichtmann, 2005). The model is thoroughly presented in Wichtmann's habilitation Wichtmann, 2016); here, I will only outline the most important computational steps for

The basic principle of the HCA model is to combine the increment-based ($\dot{\sigma} - \dot{\varepsilon}$) advanced implicit material model and the cycle number – permanent deformation ($N - \varepsilon^{acc}$) explicit model, whis is presented in 2.1. Figure.

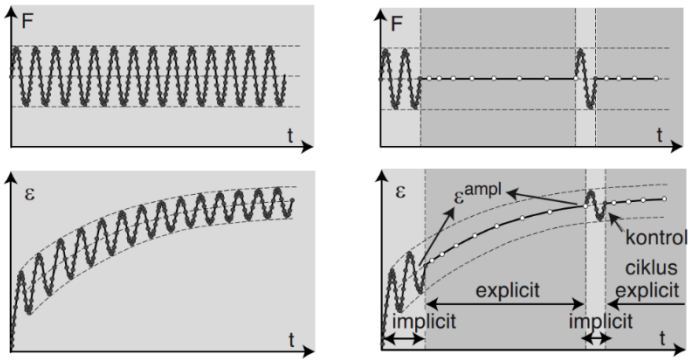

2.1. Figure: a) pure implicit method b) mixed method of the HCA model (Wichtmann, 2016)

In the first step, the strain amplitude ε^{ampl} is determined due to q^{ampl} in a traditional implicit way, which is to be interpreted as the vector sum of the vertical and horizontal strains . Then, using the strain amplitude as input parameter, the incremental residual deformation is determined with the explicit model (2.1). In the case of drained conditions, if the mean stress does not change and no plastic deformation occurs in the static sense, equation (2.1) directly provides the increment of plastic deformation

$$\dot{\varepsilon}^{acc} = f_{ampl}\, \dot{f}_N\, f_e\, f_p\, f_Y \tag{2.1}$$

The incremental residual deformation resulting from the ΔN cycle package, given a constant ε^{ampl}, is provided by equation (2.2). Since changes occur over the long term in the soil structure and state characteristics, the explicit calculation is occasionally interrupted. During these so-called control cycles, the implicit analysis is repeated to continue the explicit calculation with the updated value of ε^{ampl} for additional ΔN cycle.

$$\Delta\varepsilon^{acc} = \dot{\varepsilon}^{acc} \cdot \Delta\mathrm{N} \tag{2.2}$$

The HCA model gives the rate of accumulation as a vector quantity, so in addition to the scalar magnitude of the strain, a flow rule is also needed to specify the direction of accumulation (**m**), i.e. to specify the deviatoric ε_q and volumetric ε_v parts of the strain. These can be used to determine the vertical strain components needed for the settlement analysis.

$$\dot{\boldsymbol{\varepsilon}}^{\boldsymbol{acc}} = \dot{\varepsilon}^{acc}\boldsymbol{m} \tag{2.3}$$

In my research, I applied the MCC flow rule to the subgrade according to the findings of (Wichtmann et al., 2014b). Investigations on crushed stone base layers (Wichtmann et al., 2010) have shown that, unlike sand, the material behaves anisotropically under compaction, so the MCC flow rule does not apply. For the crushed stone base layer and the improvement layer, we used the anisotropic flow rule presented in those studies.

The scalar part of the accumulated deformation increment vector described by equation (2.1) is given as the product of 5 empirical functions f_i. These functions describe the main influencing parameters in the following order: the (elastic) strain amplitude $f_{ampl,}$ the number of cycles or the cyclic strain history $\dot{f}_N$, the void ratio f_e, the mean normal stress f_p and the stress state f_Y. The aforementioned 5 functions f_i can be described with 7 material constants C_i. Additionally, for the description of the flow rule and f_Y one needs the critical friction angle φ_{cc} which does not necessarily match the critical friction angle φ_c computed from a monotonic CU triaxial test. For determining the critical friction angle φ_{cc} for the cyclic flow rule, we used the recommendations provided in (Wichtmann et al., 2014)

I determined the HCA parameters according to the simplified calibration procedure presented in (Wichtmann et al., 2015; Wichtmann and Triantafyllidis, 2015), which applies to clean, subgranular quartz sand-gravel soils. The correlations are valid within the following limits: $1.5 < C_U < 8.0$ and $0.1\ mm < d_{50} < 3.5\ mm$, with a maximum number of cycles of $N_{max} = 2\ 10^6$.. The 2 million cycles applied in the laboratory are considered the upper limit for technical reliability. However, pavement structures may experience higher numbers of repetitions. Since we do not know the soil behavior beyond 2 million cycles, any conclusions about this range should be treated with appropriate caution and scrutiny, as we cannot be certain that the C_i parameters remain valid for $N > 2\ 10^6$.. The HCA parameters for the crushed stone base layer and the improvement layer were selected according to (Wichtmann et al., 2010).

2.2 Calculation method

In my research, I examined the settlements of pavement structures using a layered calculation method. The simplified calculation model discretizes the soil by dividing it into sublayers, analogous to conventional settlement calculation methods. We first determine the stress distribution resulting from the axle and wheel loads and establish the additional vertical stress on each sublayer, $\Delta\sigma_{1,i}$. Using this, along with the average normal stress, compaction, and deformation-dependent non-linear stiffness, we calculate the deformations ε_i^{ampl} at the midpoint of each lamella (as the average of the lamella's upper and lower parameters). Subsequently, using ε_i^{ampl} as an input parameter, we determine the accumulated deformations ε_i^{acc} for each sublayer. The settlements for each sublayer are then computed using its thickness and the cyclic flow rule as $s_{1,i}^{acc} = m_1 * \varepsilon_i^{acc\ i} * d_i$. The total settlement is the sum of the settlements for all sublayers, $\Sigma s_{1,i}^{acc}$. The principle of the layered method calculation is illustrated in Figure 2.2. Comparative finite element studies show that the simplified calculation method provides sufficiently accurate and reliable results for both elastic and residual deformations. At the end of the service life, the expected residual settlements show a difference of at most 2-7% between the simplified method and the finite element calculation method, depending on the subsoil and load class.

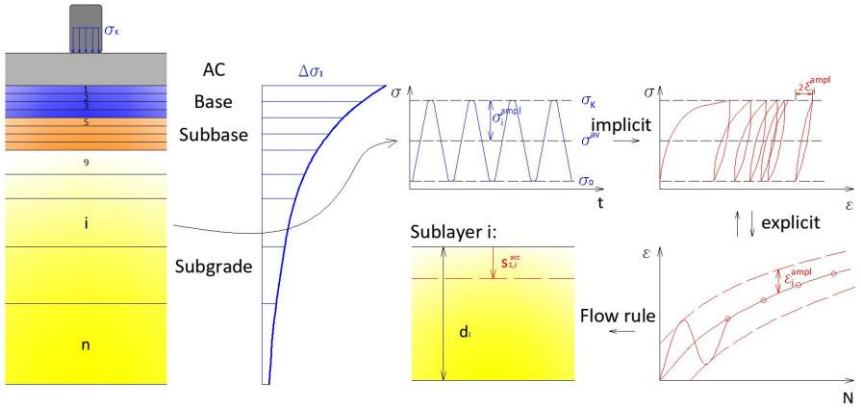

2.2. Figure: The main calculation steps of the simplified layered model (Vámos and Szendefy, 2023a)

2.3 Investigated pavement structures

The goal of this research was to determine the accumulated permanent strains and settlements in the standardized pavement cross-section according to (e-UT 06.03.13:2005, n.d.) shown in 2.1. Table due to repeated passes of a standard axle. The cross-sections are composed of 4 layers (sand and gravelly sand subgrade course, granular subbase course, crushed stone base course and asphalt course). The subgrade comprises quartz sand and gravelly sand of subangular particles; particle size distribution is shown in 2.3. Figure, and it was assumed to have a relative compaction of R.C.=93%. The subgrade is overlain by a subbase course of 20 cm thickness, which has a relative compaction of R.C.=95%. The subbase is overlain by an unbound well graded crushed stone base course of 20 cm thickness. Particle size distribution of the pavement layers is shown in 2.3. Figure, whereas their properties are summarized in 2.2. Table. The base course is overlain by an asphalt course of traffic load class-dependent thickness.

2.1. Table Standardized pavement cross-sections accordig to (e-UT 06.03.13:2005)

Traffic load class						
A	B	C	D	E	K	R
Design traffic (million axles)						
0,03-0,1	0,1-0,3	0,3-1	1-3	3-10	10-30	30 felett
Cross secvtion with crushed stone base course						
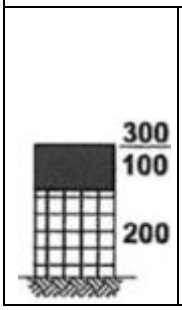	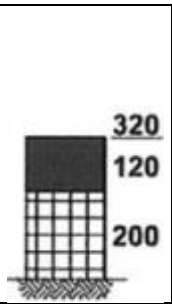	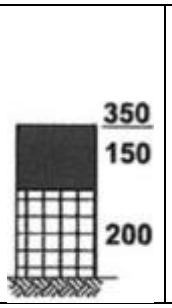	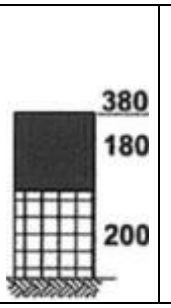	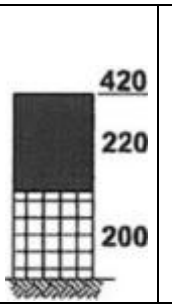	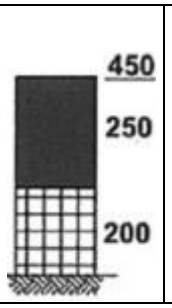	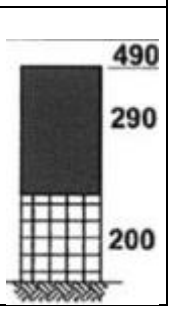

2.4 Investigated soils and their material properties

For the subsoil, I selected sands and sandy gravels. The reason for this choice is that reliable literature data for HCA parameters is most readily available for these types of soils. In my research, I examined 5 different subgrade types, which cover the spectrum of soils that can be investigated using the simplified calibration procedure presented in (Wichtmann et al., 2015; Wichtmann and Triantafyllidis, 2015). I investigated the effect of the mean grain diameter using soils with "Subgrade 1", "Subgrade 2", and "Subgrade 3" grain size distributions, where I varied the d_{50} value (0.2 mm, 0.6 mm, and 2.0 mm) while keeping the inequality index constant (C_U = 3). The effect of the coefficient of uniformity was examined using soils named "Subgrade 3", "Subgrade 4", and "Subgrade 5", where I varied C_U values between 3.0, 5.0, and 8.0, while keeping d_{50} constant at 0.6 mm. The grain size distribution diagrams of the examined soils are shown in Figure 2.3.

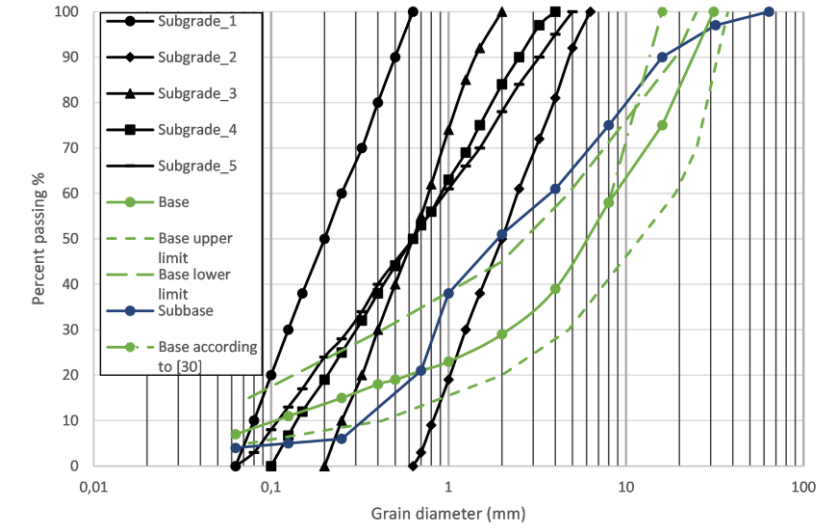

2.3. Figure: Particle size distribution of the pavement layers

2.2. Table: geotechnical parameters of the modelled layers

Layer	d_{50} (mm)	C_u (-)	e_{min} (-)	e_{max} (-)	ρ_d^{max} (g/cm^3)	e_0 (-)	υ (-)
Subgrade 1	0,2	3,0	0,540	0,920	1,75	0,627	0,33-0,36
Subgrade 2	2,0	3,0	0,491	0,783	1,81	0,577	0,33-0,36
Subgrade 3	0,6	3,0	0,474	0,829	1,83	0,559	0,33-0,36
Subgrade 4	0,6	5,0	0,394	0,749	1,93	0,478	0,35-0,38
Subgrade 5	0,6	8,0	0,356	0,673	1,98	0,439	0,36-0,40
Subbase	2,0	11,9	0,364	0,513	2,06	0,340	0,40
Base	6,3	100,0	0,230	0,440	2,30	0,188	0,40

In my research, for implicit calculations, I considered the subgrade as nonlinearly elastic, taking into account the average normal stress, void ratio, and small strains. I determined the maximum shear modulus G_{max} and the compressibility modulus using correlations dependent on d_{50} and C_u, as described in (Wichtmann and Triantafyllidis, 2009) and (Wichtmann and Triantafyllidis, 2010). The degradation curve was established using CU-dependent relationships outlined in (Wichtmann and Triantafyllidis, 2013). Since the stiffness (G, E, M, υ) also depends on average normal stress and deformation, it must be determined for each sublayer, in every cycle package, and for each load increment, as it continuously changes. Additionally, the actual strain increment and the corresponding actual stiffness must be determined through iteration for each loading step. The stiffness of the crushed stone base layer and improvement layer was considered with the resilient modulus based on Table 5-30 from (AASHTO, 2002).

2.5 Calibration and comparison of own results with other methods

In the first step, I conducted comparative studies using the Plaxis finite element software to obtain input data regarding the distribution of horizontal strains and stresses, and to verify the adequacy of the cyclic strain amplitude resulting from my own calculation procedure. Following this, I examined the effect of the HS-Small material model's $\gamma_{0,7}$ parameter and then conducted investigations into the construction of the laminar method. Finally, I presented the validation of the residual settlements determined by the computational procedure, comparing them with other methods. Through this process, I confirmed that the calculation procedure I developed shows good agreement with finite element comparative calculations for both resilient strains and accumulated residual deformations. The comparative studies revealed that the embankments of the examined standard cross-section, especially in higher loading classes, do not meet international standards. Consequently, it is anticipated that excessive pavement structure settlements may occur, particularly in higher loading classes. Comparative settlement calculations show that, despite slightly differing boundary conditions, the results of my settlement calculations align well with other methods. The orders of magnitude are nearly identical, and the nature of the curves is quite similar.

3 NEW SCIENTIFIC RESULTS

1. New scientific result

In my research, I developed a simplified layered calculation procedure in Excel, which first determines for granular soil layers beneath the flexible pavement structures the cyclic strain amplitude ε^{ampl} using an implicit calculation method. Then by using using an explicit method with the HCA model my calculation procedure determines the accumulated residual strains ε^{acc} and settlements s^{acc} induced by cyclic traffic loads. To provide input data for my calculation procedure regarding the distribution of horizontal strains and stresses, and to verify the adequacy of the cyclic strain amplitude resulted from my own method, I conducted comparative studies using the Plaxis finite element software.

1.1. New scientific result

I found that the loads from construction traffic and compaction significantly exceed the operational loads, resulting in overconsolidated soils beneath the pavement structures, with OCR >> 1, consequently, $K_{xy} \neq K_0^{NC}$. Based on finite element calculations, I determined the stress distributions in the crushed stone base layer, subbase layer, and subgrabe beneath the standard cross-sections of traffic load class "A"-"R". **Using these results, I established the spatial distribution of the K_{xy} earth pressure coefficient as a function of depth and load magnitude, taking into account the overconsolidation due to construction conditions. I provided recommendations indicating that the earth pressure coefficient in the crushed stone base layer can be described using the function (3.1) and the parameters specified in Table 3.1.**

$$K_{xy}^{base}(z) = K_{xy,max}^{base} - (z\frac{K_{xy,max}^{base} - K_{xy,min}^{base}}{d_{base}}) \quad (3.1)$$

3.1. Table: Earth pressure coefficient at the top ($K_{xy,max}^{base}$) and at the base ($K_{xy,min}^{base}$) of the crushed stone base course

Coefficient of earth pressure	Independently of traffic load class
$K_{xy,max}^{base}$	0,85
$K_{xy,min}^{base}$	0,10

I made recommendations that the earth pressure coefficient in the subbase layer can be described using the constants specified in 3.2. Table:

3.2. Table: Coefficient of earth pressure (K_{xy}^{sb}) in the subbase course in the function of traffic load class and wheel load

Traffic load class	Load step					
	0 t	2 t	4 t	6 t	8 t	10 t
	K_{xy}^{sb}					
A	6,55	2,33	1,06	0,52	0,26	0,23
B	6,14	2,66	1,19	0,63	0,32	0,19
C	6,02	2,51	1,34	0,79	0,47	0,28
D	5,90	2,95	1,74	1,11	0,74	0,50
E	5,93	3,26	2,13	1,51	1,11	0,84
K	5,11	3,43	2,41	1,79	1,38	1,08
R	5,65	3,55	2,62	2,03	1,63	1,33

I made recommendations that the earth pressure coefficient in the subgrade can be described using the function (3.2) and the parameters specified in Table 3.3.

$$K_{xy}^{sg}(z) = \begin{cases} K_{xy,top}^{sg} - \left[(z - d_{base} - d_{sb})\frac{K_{xy,top}^{sg} - K_{xy,max}^{sg}}{1{,}0}\right], & d_{base} + d_{sb} \le z \le d_{base} + d_{sb} + 1{,}0 \\ K_{xy,max}^{sg} - \left[(z - d_{base} - d_{sb} - 1)\frac{K_{xy,max}^{sg} - K_{xy,bottom}^{sg}}{d_{sg} - 1}\right], & d_{base} + d_{sb} + 1 < z \end{cases} \quad (3.2)$$

3.3. Table: Coefficient of earth pressures in the sand subgrade

Coefficient of earth pressure	Regardless of load class
$K_{xy,top}^{sg}$	0,55
$K_{xy,max}^{sg}$	0,94
$K_{xy,bottom}^{sg}$	0,62

The earth pressure coefficients K_{xy} in the crushed stone base layer and subbase layer, as determined by finite element calculations, and their approximations according to equation (3.1) and Table 3.1, are illustrated in Figure 3.1. The earth pressure coefficients K_{xy} in the subgrade, as determined by finite element calculations, and their approximations according to equation (3.2) and Table 3.3, are illustrated in Figure 3.2.

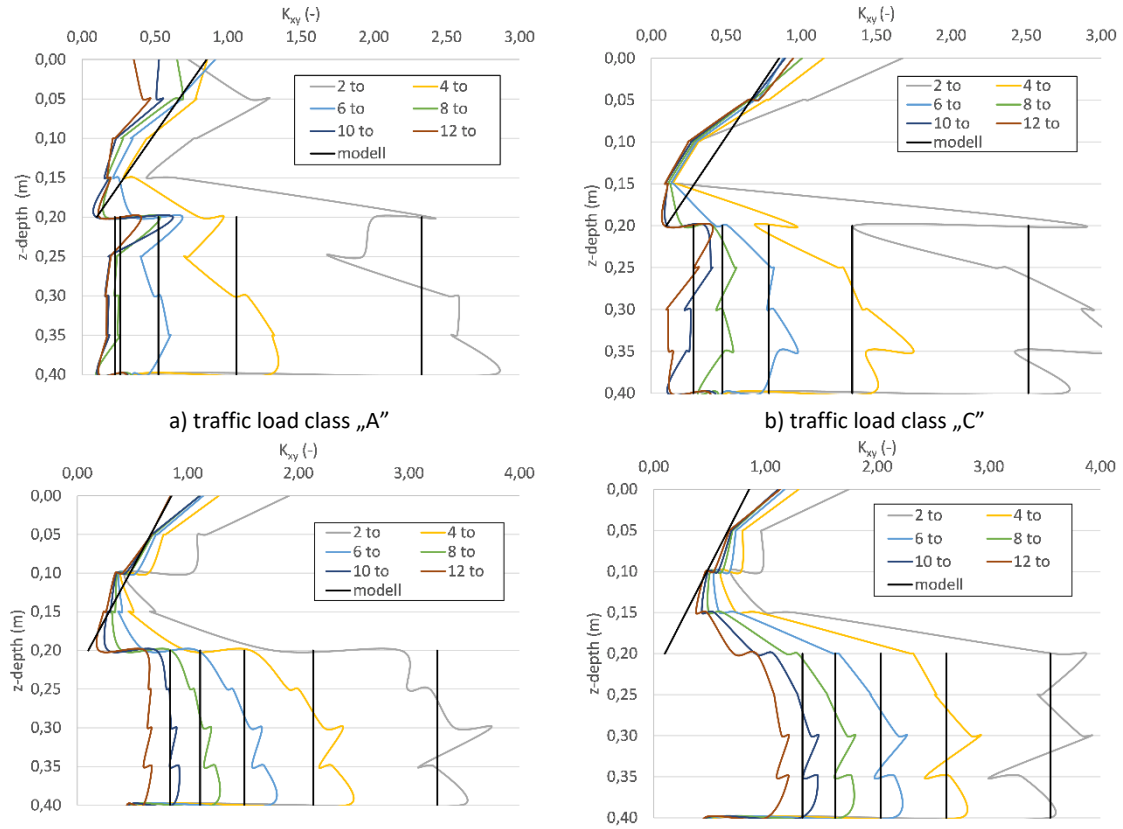

a) traffic load class „A”

b) traffic load class „C”

c) traffic load class „E”

d) traffic load class „R”

3.1. Figure Coefficients of earth pressure in the base and subbase courses asobtained from the finite element modelling and approximation of them

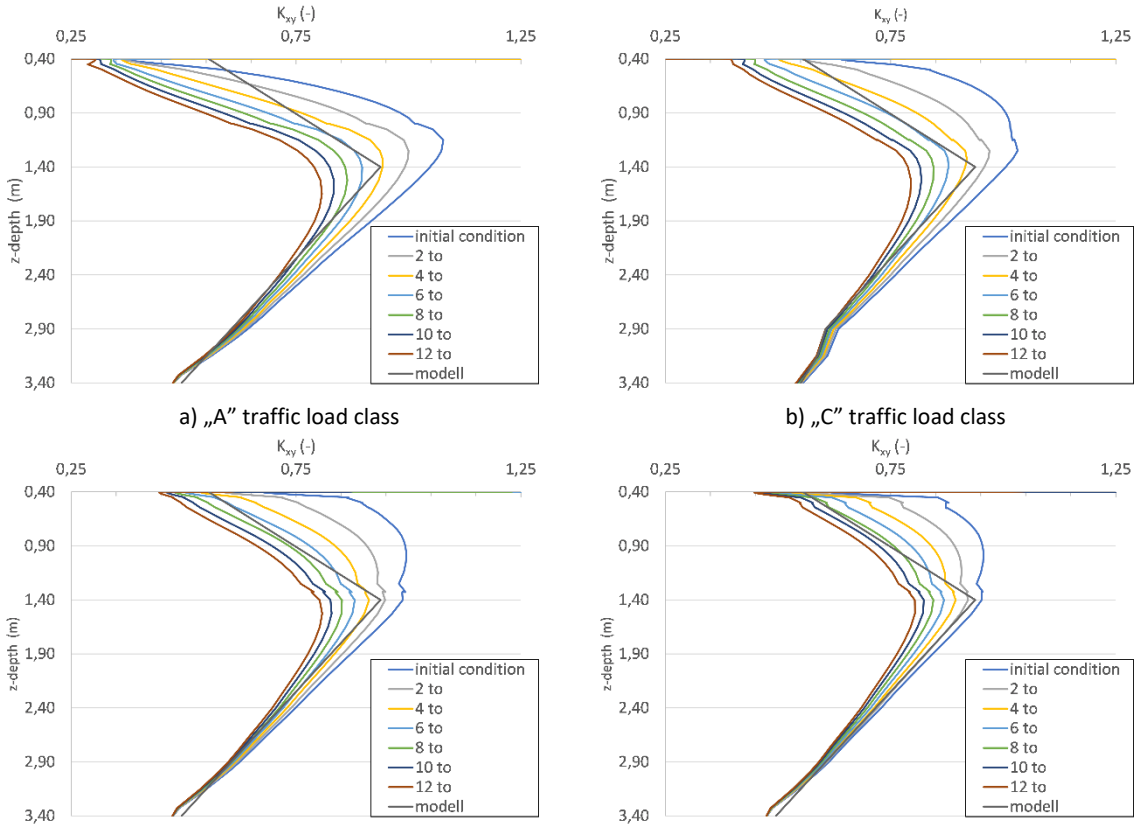

a) „A” traffic load class

b) „C” traffic load class

c) „E” traffic load class

d) „R” traffic load class

3.2. Figure Coefficients of earth pressure in the subgrade as obtained from the finite element modelling and approximation of them

1.2. New scientific result

Based on finite element calculations, I determined the strain conditions in the crushed stone base and subbase layer, and subgrade beneath the standard cross-sections "A"-"R". **Using these results, I calculated the ratio of horizontal to vertical strains as a function of depth and load magnitude. Finite element calculations confirmed that the typical behavior observed for conventional soil masses is only approximately valid for the subgrade, with significant deviations in the crushed stone base and subbase layers, which can be explained by the plate-like behavior of these courses. I made recommendations that the ϑ factor can be described using the function (3.3) and the parameters specified in Table 3.4.**

$$\vartheta(z) = \begin{cases} \vartheta_{max,base} + \left(z \dfrac{\vartheta_{max,base} - \vartheta_{min,base}}{d_{base}}\right), & z \le d_{base} \\ \vartheta_{max,sb} + \left((z - d_{base}) \dfrac{\vartheta_{max,sb} - \vartheta_{min,sb}}{d_{sb}}\right), & d_{base} < z \le d_{sb} + d_{base} \\ \vartheta_{max,sg} + \left((z - d_{base} - d_{sb}) \dfrac{\vartheta_{max,sg} - \vartheta_{min,sg}}{0{,}75}\right), & d_{base} + d_{sb} < z \le 0{,}75 + d_{sb} + d_{base} \\ \vartheta_{min,sg}, & z > 0{,}75 + d_{sb} + d_{base} \end{cases} \quad (3.3)$$

3.4. Table: Maximum and minimum values of the horizontal and verticalstrain ratio

Layer	ϑ_{max}	ϑ_{min}
Base	0,850	-0,450
Subbase	-0,300	-0,800
Subgrade	-0,050	-0,325

The deformation ratios ϑ according to the finite element calculations, as well as their approximations using function (3.3) and Table 3.4, are illustrated in Figure 3.3.

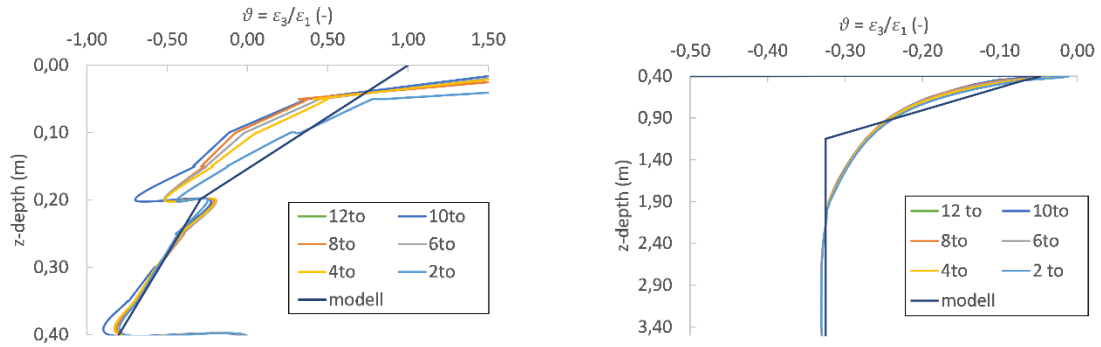

3.3. Figure: The calculated and fitted *ϑ* functions with depth a) in the base and subbase courses b) in subgrade for traffic load class C

1.3. New scientific result

I conducted investigations into the required number and arrangement of sublayers. **By varying the number of sublayers, I revealed that the necessary and sufficient numbers of sublayers for the base and subbase courses, and subgrade layers are 4, 4, and 11, respectively. Increasing the number of sublayers beyond these numbers does not lead to a significant improvement in accuracy (see Figure 3.4). For the subgrade, I demonstrated through parameter studies that, with the same number of sublayers, more accurate results are obtained by concentrating the lamellae in the upper sections rather than distributing them evenly, while using thicker sublayers for the deeper sections.**

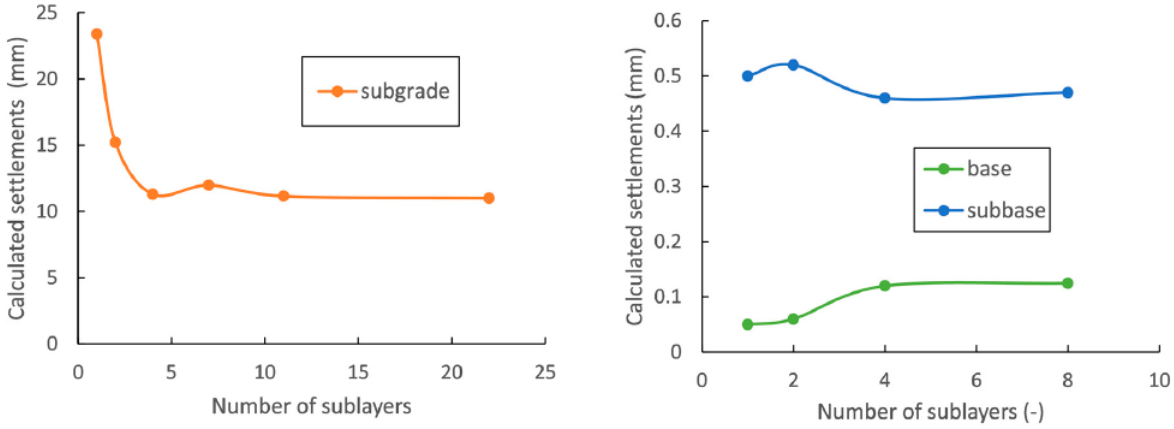

3.4. Figure: The calculated settlements as the function of number of sublayers, (a) For the subgrade and (b) for subbase and base courses.

1.4. New scientific result

The resilient behavior should be considered using a nonlinear elastic material model for soils. For the subgrade, the effects of compaction, average normal stress, and the small strains must be taken into account. For the crushed stone base and subbase layers, it is sufficient to use a pressure-only nonlinear elastic k−Θ model. **By varying the number of load increments, I determined that the necessary and sufficient number of load steps is i=40 (see Figure 3.5).**

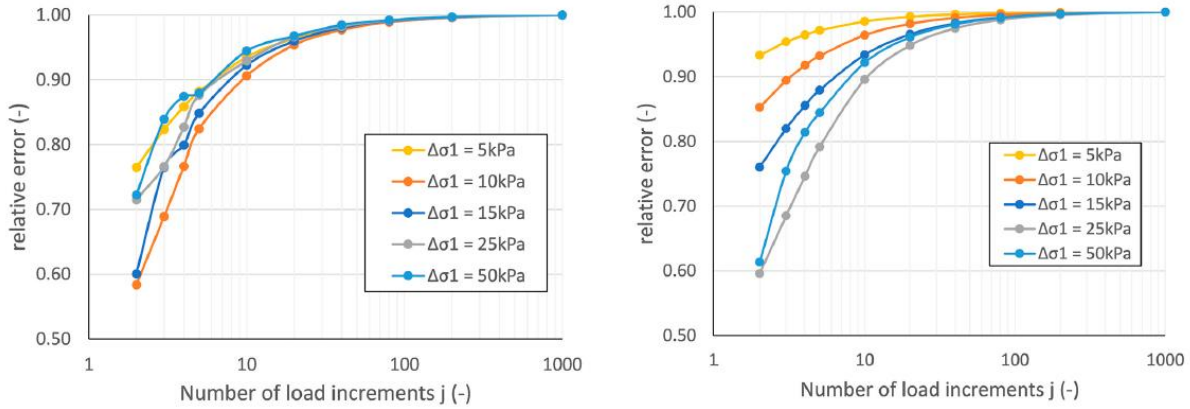

3.5. Figure The calculated relative error as the function of the number of load steps (a) at the depth of 0.5 m and (b) at the depth of 2.5 m.

Comparative calculations confirmed that the laminar calculation method I developed, which relies solely on literature-based input data (d_{50}, C_U, k_1, k_2), provides sufficiently accurate input data for cyclic strain amplitude ε^{ampl} even without finite element calculations (see Figure 3.6). According to comparative settlement calculations for the "C" traffic load class, the difference in the final values of residual deformations ranges from 3-7%, depending on whether the input data for the HCA model come from my own calculation procedure or from finite element calculations (see Figure 3.7).

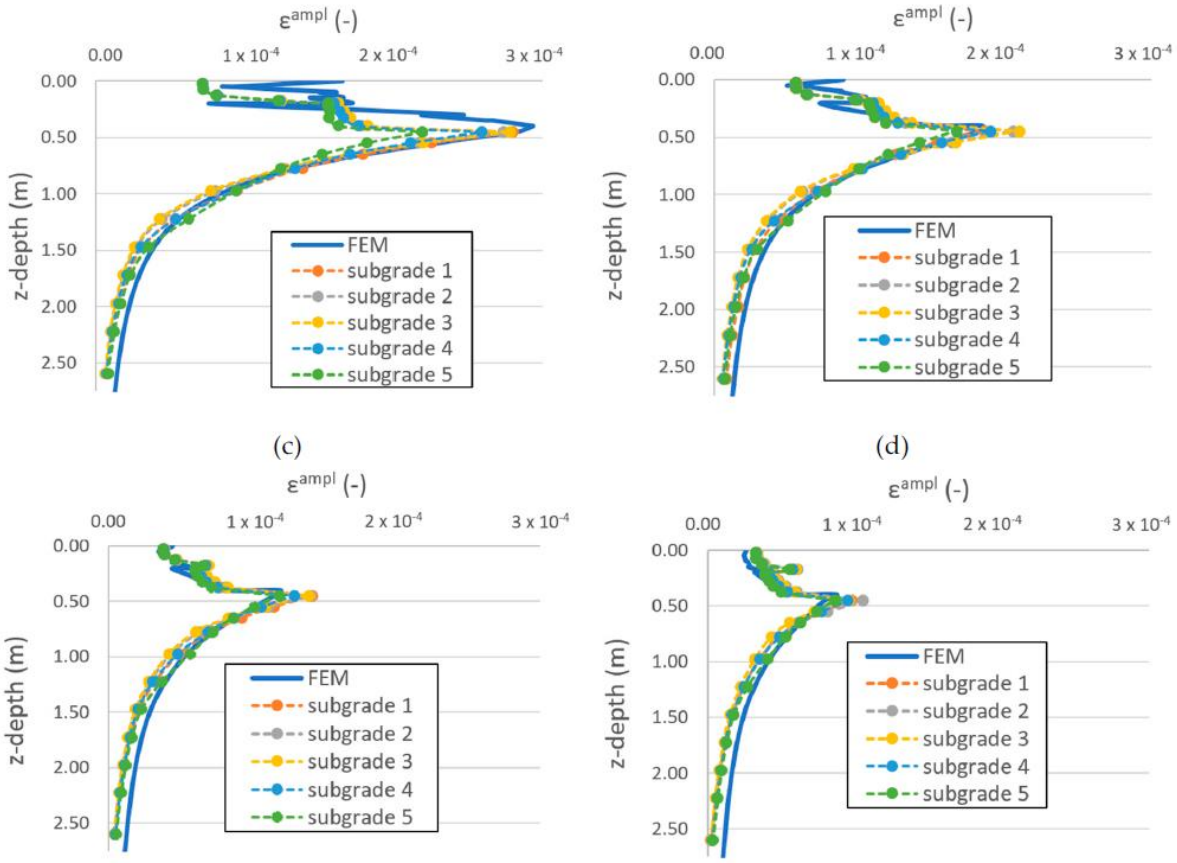

3.6. Figure: The calculated "ampl-z function with the simplified layered model for five different subgradesand with finite element model (a) Traffic load class “A”; (b) Traffic load class “C”; (c) Traffic load class “E”; (d) Traffic load class “R”

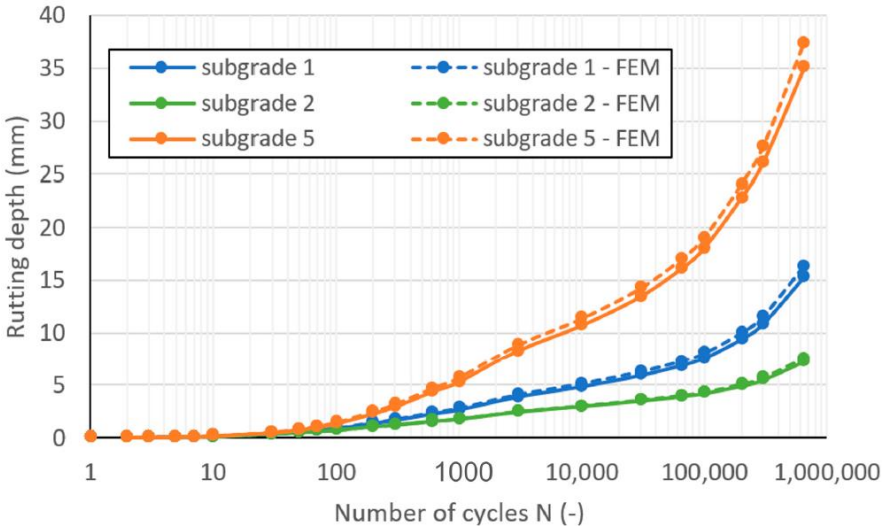

3.7. Figure: Calculated rutting depths for traffic load class “C” obtained by the simplified procedureand the finite element model for three different subgrades.

Related publications: (Vámos and Szendefy, 2023a, 2023b)

2. New scientific result

Using the presented calculation method, I determined the expected residual settlements on the top of the base layer due to the the repeated standard axle over the service life for the standard cross-sections according to e-UT 06.03.13. I examined the effect of grain size distribution parameters (C_U and d_{50}) on settlements for 5 different subgrade types. I assessed and illustrated the percentage contribution of each soil layer (base, subbase, subgradel) to the total settlements.

2.1. New scientific result

I calculated and illustrated in figures the settlements for each traffic load class at the surface of base layer for 5 different subgrade, as a function of the number of cycles. This provided the complete spectrum and temporal evolution of the expected settlements. I demonstrated that the subsoil has a decisive impact on the settlements, and I evaluated the settlement ratios between different subsoils in Table 3.5:

3.5. Table: Total settlements and their ratio for subgrades with the lower and upper bound particle size distributions

Traffic load class	Total settlement (mm)			„Subgrade-5" / "Subgrade-2"	„Subgrade-1" / "Subgrade-2"
	„Subgrade-1"	„Subgrade-2"	„Subgrade-5"		
A	11.0	5.8	20.6	3.6	1.9
B	12.5	6.4	25.2	3.9	2.0
C	15.5	7.2	35.0	4.9	2.2
D	22.8	9.1	45.6	5.0	3.2
E	33.8	16.1	56.6	3.5	2.1
K	47.1	27.4	67.5	2.4	1.7
R	50.4	32.1	68.2	2.1	1.6

The accumulted settlements determined for the 5 different subgrades are illustrated for the "D" load class in Figure 3.8, using a selected example.

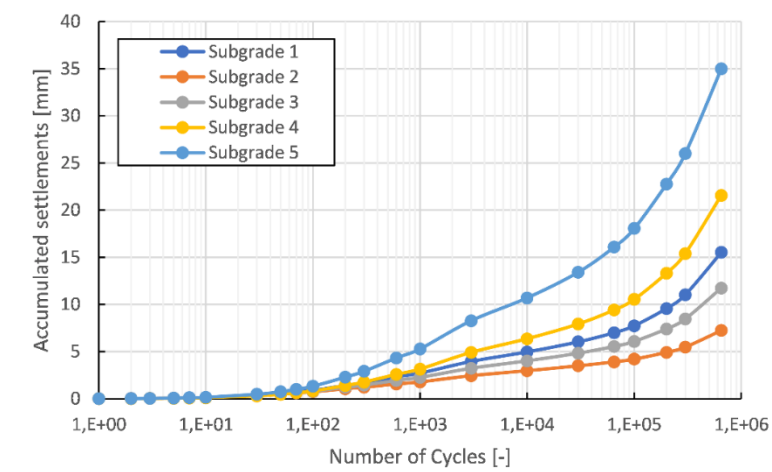

3.8. Figure: The effect of subgrade on settlements on the top of the base layer in the case of traffic load class „C"

My calculations have shown that, with a constant d_{50}, increasing C_U significantly increases the cumulative settlements. Furthermore, I found that with a constant C_U, increasing d_{50} has a beneficial effect on settlements.

2.2. New scientific result

I calculated and illustrated in diagrams the pavement structure settlements for each traffic load class at the surface of the base course, as a function of the number of cycles, for the different subsoil types. The determined accumulated settlements as a function of the number of cycles for the "Subgrade 3" are shown in Figure 3.9.

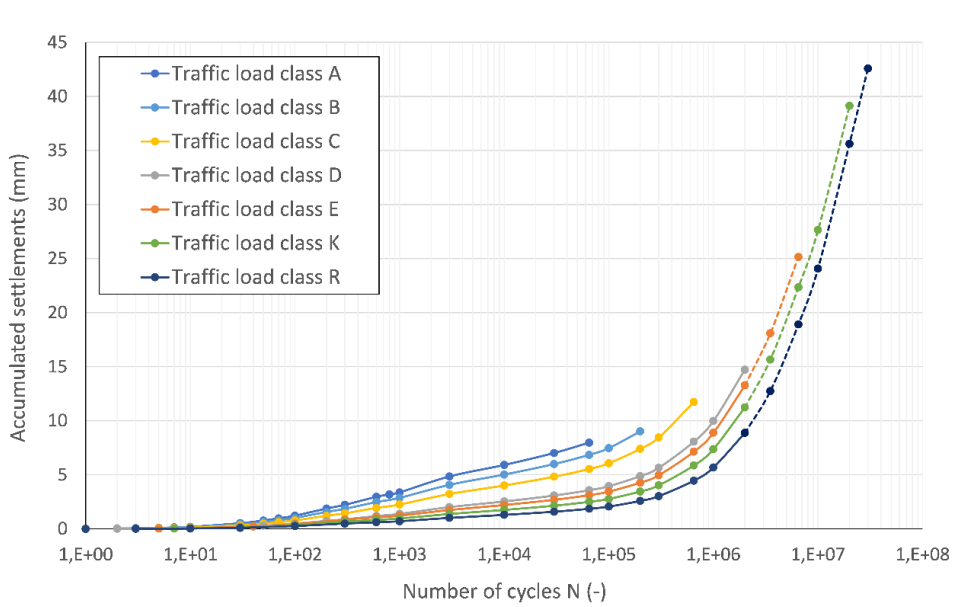

3.9. Figure: The relationship between settlement and cycle number in the case of „Subgrade-3"

I found that the calculated settlement at the end of the service life increases with the traffic load class. I demonstrated that, with unchanged boundary conditions (e.g., subgrade type) and the same number of cycles, the different traffic load classes experience proportionally larger settlements relative to the thickness of the asphalt layers, according to the relationship given in (3.4), as the normal settlement curves nearly coincide (Figure 3.10).

$$s_{i,normalized}(N) = s_i(N) / \left(\frac{d_{asphalt,i}}{d_{asphalt,R}}\right)^{1.3} \tag{3.4}$$

Where, $s_{i,normalized}(\mathrm{N})$ normalized settlements
$s_i(N)$ calculated settlements
$d_{aszfalt,i}$ thickness of asphalt in the traffic load class „i"
$d_{aszfalt,R}$ thickness of the asphalt in the traffic load class „R"

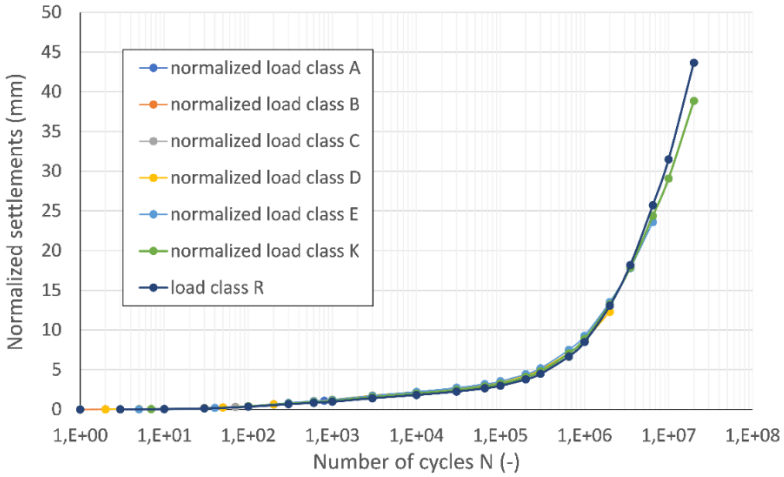

3.10. Figure: Normalized settlements on the surface of the base layer with the thickness of the asphalt

2.3. New scientific result

I calculated, plotted, and evaluated the percentage contribution of each course to the total settlements for the A-C-E-R traffic load classes and for the "subgrade 1"-" subgrade 2"-" subgrade 5" subsoil types. I found that a significant portion of the settlements originates from the subgrade (75% - 98%). I established that by the end of the load, the proportion of the subgrade in the total settlements decreases, and generally decreases with increasing traffic load class. I also found that soils with better gradation and easier compactability contribute more to the settlements than soils with steep particle size distributions.

The contribution ratios of the individual structural layers to the total settlements for the A-C-E-R traffic load classes, specifically for “subgrade 5” and “subgrade 2,” are illustrated in Figures 3.11 and 3.12.

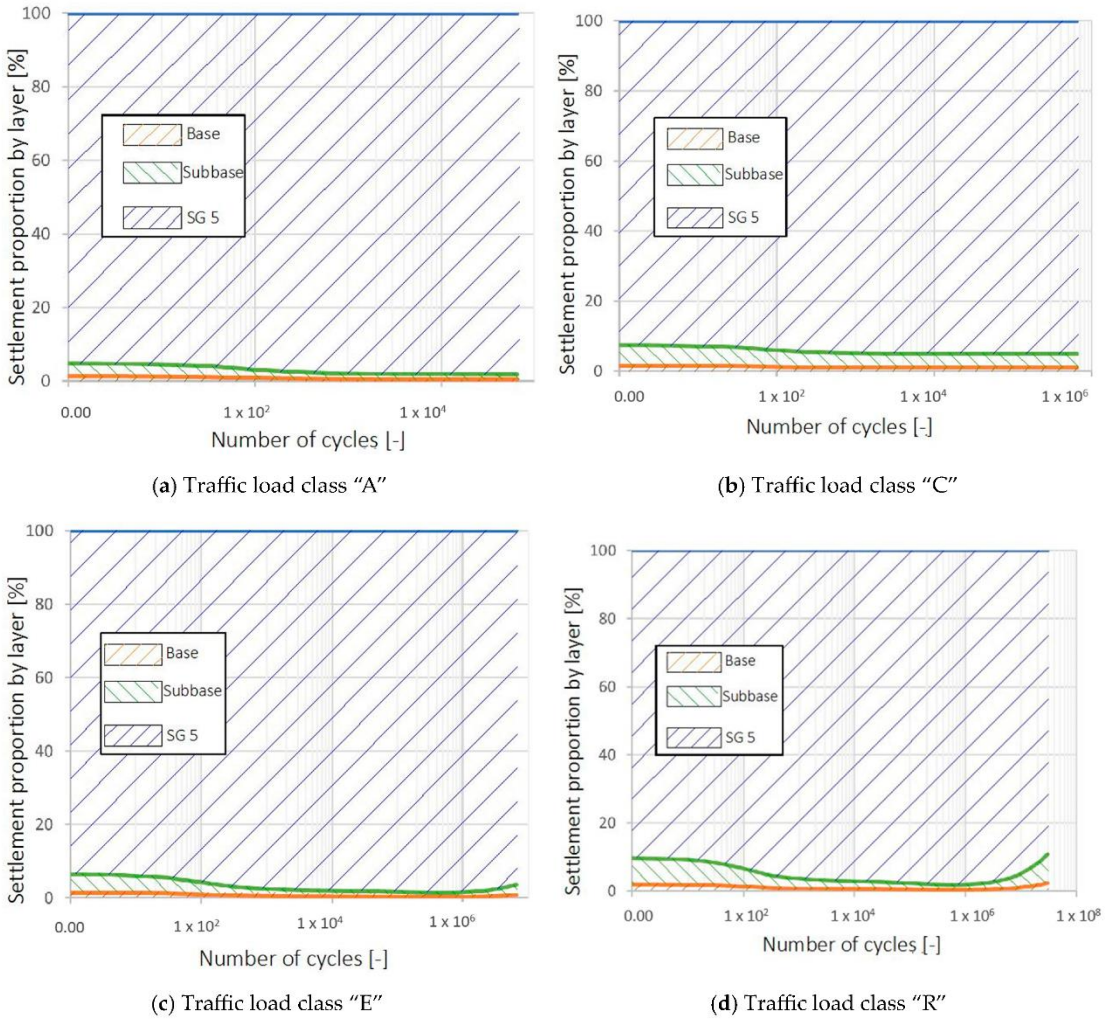

(a) Traffic load class “A”

(b) Traffic load class “C”

(c) Traffic load class “E”

(d) Traffic load class “R”

3.11. Figure: The contribution of each layer to the total settlement as a function of the number of cycles – „Subgrade-5”

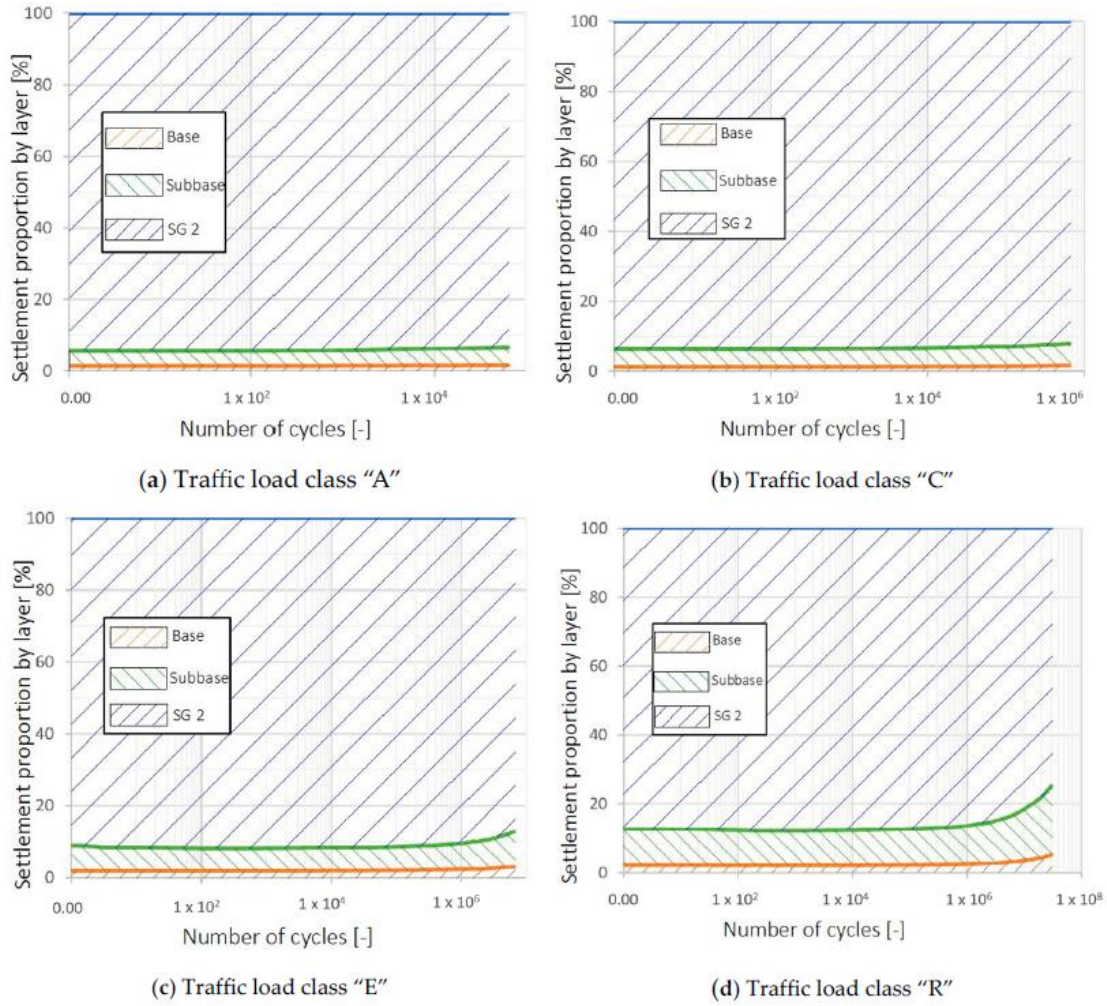

3.12. Figure: The contribution of each layer to the total settlement as a function of the number of cycles— "Subgrade-2".

Related publications: (Vámos and Szendefy, 2024a)

3. New scientific result

To determine the relative settlement differences of the pavement structure and the maximum additional tensile strains that could potentially arise in the asphalt from the deformed soil, I conducted an analyzis and calculated the settlement depression and the planar extent of settlements interpreted at the surface of the base course. For this purpose, using the HCA model, I determined the accumulated strains and settlements in cross-sections that differ from the wheel's symmetry axis, while also taking into account the interaction with neighboring tires.

3.1. New scientific result

I analyzed the settlement depression curve interpreted at the surface of the base layer for the "C" traffic load class and the representative "subgrade 1" - " subgrade 2" - " subgrade 5" soil types, and computed the relative settlement differences of the pavement structure. Calculations confirmed that the impact of the subgrade on the relative settlement differences of the pavement structure is significant, and the trend regarding settlements calculated at the wheel axis remains consistent, although the ratios between different soil types are slightly balanced, see Figure 3.13 and Table 3.6.

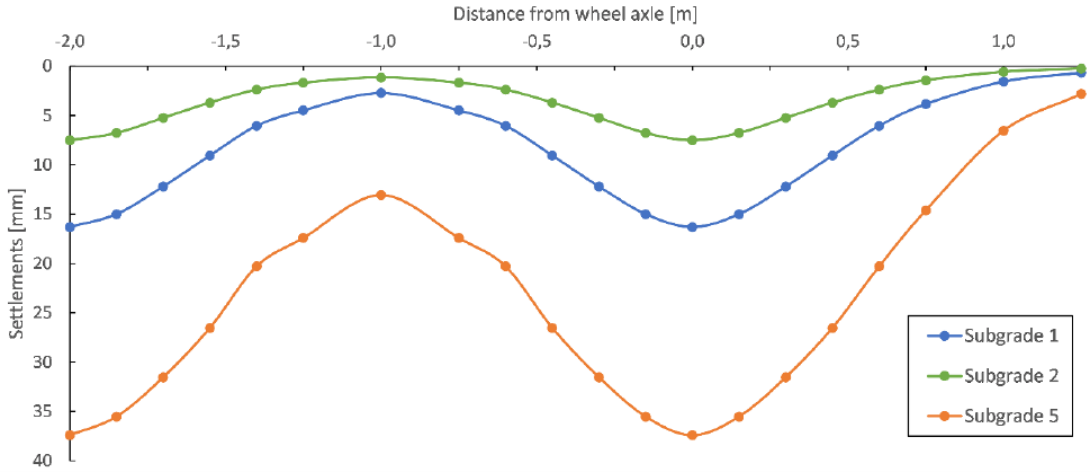

3.13. Figure: Settlement depressions for traffic load class „C" and „Subgrade-1", „Subgrade-2" and „Subgrade-5"

3.6. Table: Rut depth and settlement difference calculated for traffic load class „C"

Subgrade	D_0 (x = 0 m) (mm)	D (x = -1,0 m) (mm)	Relative settlement difference (mm)
Subgrade 1	16.30	3.11	13.19
Subgrade 2	7.51	1.15	6.36
Subgrade 5	37.40	13.06	24.34

3.2. New scientific result

I determined the settlement depression curves interpreted at the surface of the base course for the A-C-E-R traffic load classes and a specified subgrade, and computed the relative settlement differences of the pavement structure (Figure 3.14). I found that the settlement increase in the A-C-E traffic load classes, but despite a significantly increasing absolute settlement in the R class, there is no substantial increase in the relative settlement difference. I concluded that this is due to the better load distribution effect of the thicker asphalt layer.

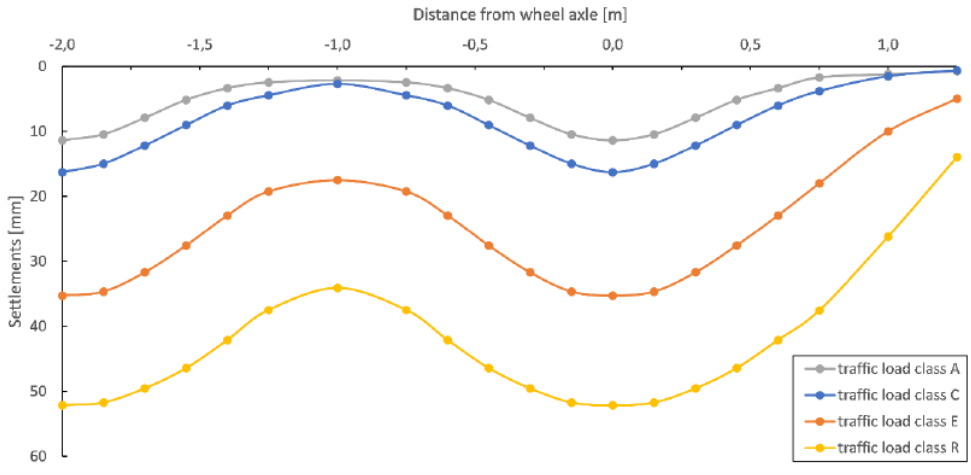

3.14. Figure: The calculated depression curves for different traffic load classes in the case of „Subgrade-1"

3.7. Table: The calculated rut depth for different traffic load classes in the case of „Subgrade-1"

Traffic load class	D_0 (x = 0 m) (mm)	D (x = -1,0 m) (mm)	Relative settlement difference (mm)
„A"	11.37	2.19	9.18
„C"	16.30	3.11	13.19
„E"	35.26	17.53	17.73
„R"	52.12	34.09	18.03

3.3. New scientific result

The settlement depression curve can be described using the function for deformation measurement proposed by (Primusz and Tóth, 2009). **I have demonstrated that the possible maximum strain of the asphalt edge,**

derived from the calculated plastic deformations, significantly exceeds the stresses resulting from elastic deformation. Recommendations have been made for the shape factors of the settlement depression curve for different load classes and soil types (Tables 3.8 and 3.9):

3.8. Table: Calculated possible maximum asphalt strain, curvature radii, and settlement depression curve shape factors for the 'C' load class

Subgrade	ε_{xx} (microstrain)	R_0 (m)	c (-)
Subgrade 1	10.798	6,95	0,397
Subgrade 2	6.587	11,39	0,526
Subgrade 5	15.672	4,79	0,251
Resilient	142	526,59	0,255

3.9. Table Calculated possible maximum asphalt strain, curvature radii, and settlement depression curve shape factors for „subgrade 1”

Traffic load class	ε_{xx} (microstrain)	R_0 (m)	c (-)
„A”	7.046	7,09	0,557
„C”	10.797	6,94	0,397
„E”	14.496	7,58	0,168
„R”	13.867	10,45	0,083

3.4. New scientific result

I developed a simplified sizing procedure that estimates the possible maximum additional asphalt elongation and the structural settlement differences resulting from plastic deformations. The procedure for this sizing method is illustrated in Figure 3.15:

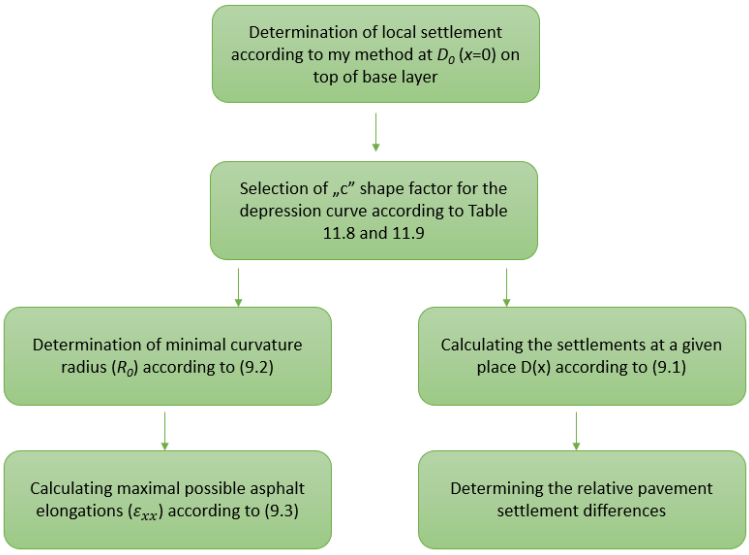

3.15. Figure: Simplified sizing procedure for determining possible maximum additional asphalt stresses and structural settlement differences resulting from subsequent soil compression

Related publications: (Vámos and Szendefy, 2024b)

4. New scientific result

4.1. New scientific result

I conducted investigations on the standard cross-section 'C', with axle loads varying between 2-4-6-8-10-12 tons, and **calculated the expected spectrum of settlements on the surface of the base layer as a function of the number of cycles, as shown in Figure 3.16.**

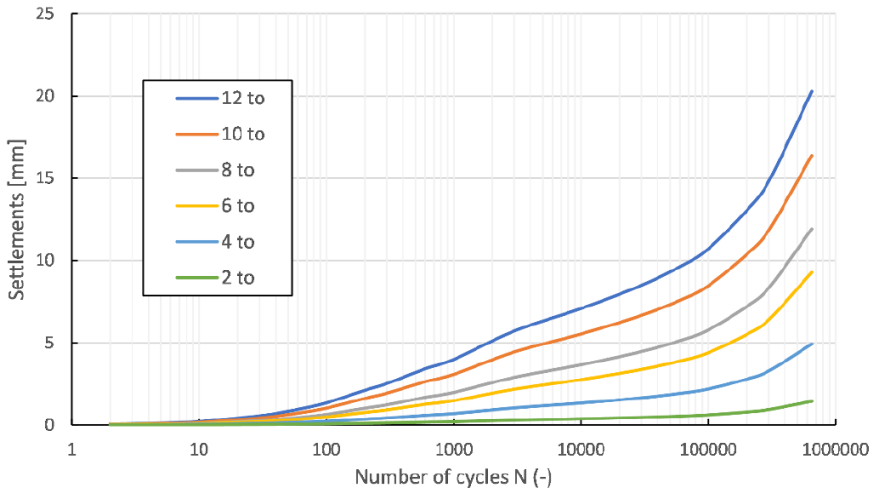

3.16. Figure: Settlements as a number of cycles for different axle loads in the case of traffic load class „C" and „Subgrade-1"(Vámos and Szendefy, 2024b)

I demonstrated that reducing the axle load decreases the depth of the subsoil zone affecting the settlements. I also showed that, with a constant number of cycles, the calculated settlements increase directly in proportion to the axle load (Figure 3.17).

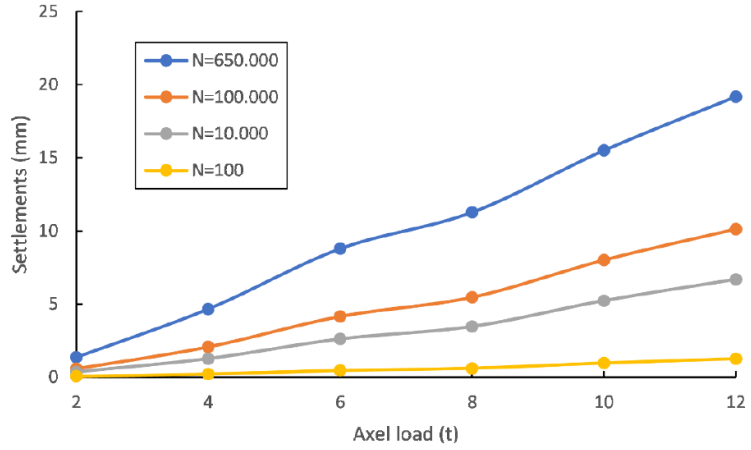

3.17. Figure: Calculated settlement as a function of the axle load for different cycle numbers (Vámos and Szendefy, 2024b)

I determined for various 2-4-6-8-10-12 ton axle loads the required number of cycles for a settlement equivalent to the standard axle load and design traffic (Table 3.10).

3.10. Table: Cycle numbers causing the same amount of settlement as the standard axle load and their ratio

Axle load (t)	2	4	6	8	10	12
$N_{required}$	13 750 000	4 450 000	1 850 000	1 235 000	650 000	385 000
N_i/N_{10to}	21,15	6,85	2,85	1,90	1,00	0,59

I provided an equation for the required number of cycles for a given axle load causing settlements equivalent to the standard axle load, with R^2 = 0.971

$$N_{required} = e^{16.884 - \frac{axle\ load\ (t)}{2.826}} \quad (3.5)$$

Where, $N_{required}$ the required number of axle passes
e the Euler number

4.2. New scientific result

I examined the effect of the thickness of the subbase layer on the settlements calculated at the wheel axle on the surface of base layer for the 'E' load class and subgrade 1. **My calculations demonstrated to what extent increasing the thickness of the subbase layer can reduce the accumulated settlements (Figure 3.18)."**

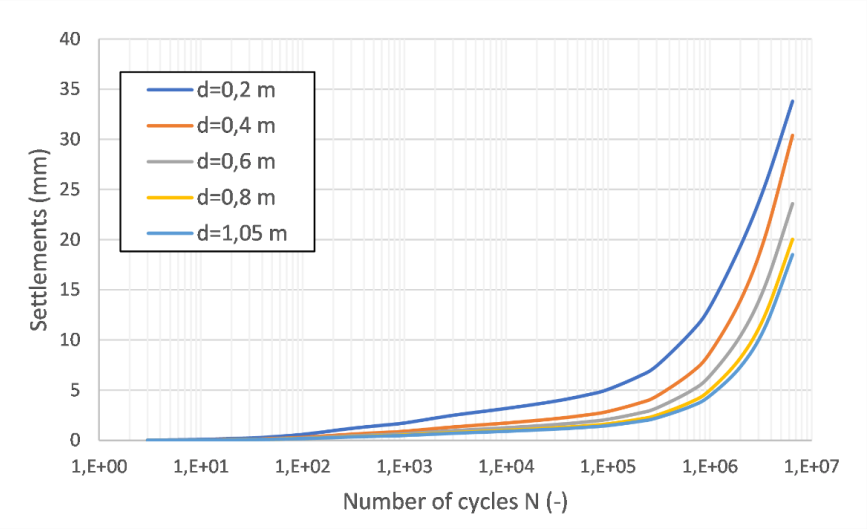

3.18. Figure: Settlement as a function of cycle number for different subbase thicknesses in the case of traffic load class „E" and „Subgrade-1"

I established that from an economic perspective, a thickness greater than d=0.8 m does not achieve a significant reduction in settlements (Figure 3.19):

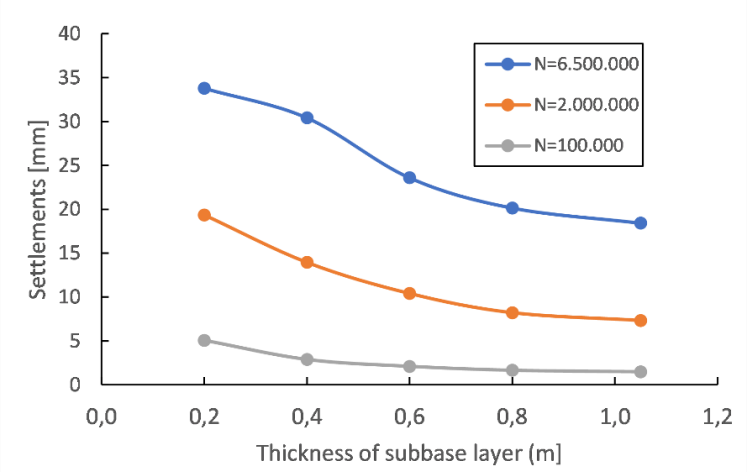

3.19. Figure: Calculated settlements as a function of the subbase thickness for different cycle numbers

I performed an analysis on the impact of the material and the quality characteristics of the aggregate shape of the subbase on settlements. I examined crushed stone aggregate, naturally rounded aggregate, and a 50%-50% mixed ratio material. **My calculations revealed that the quality of the subbase has a significant effect on settlements, with nearly twice the difference in settlements between crushed and rounded aggregates (Figure 3.20):**

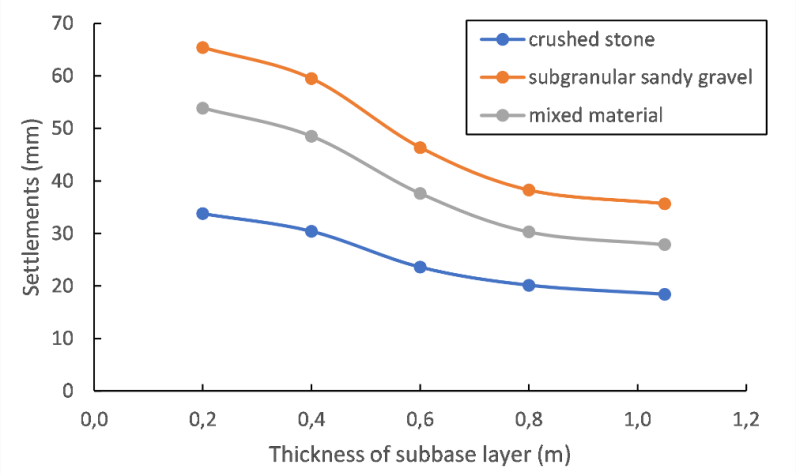

3.20. Figure: Calculated settlements as a function of the subbase thickness for the analysed materials

A subbase with rounded material experiences greater settlements even at a thickness of d=1.05 meters compared to the d=0.2 meter thick crushed stone aggregate. **Based on this, I recommended that, for effective reduction of settlements and relative settlement differences, not only the thickness of the subbase layer but also the use of high-quality crushed stone aggregate with angular grain shape is essential.**

4.3. New scientific result

I carried out studies on the effects of seasonal temperature fluctuations on the settlement on the surface of the base course with varying stiffness. In this study, I examined the "C" load class and the subgrade 1. In the calculations, I first analyzed the "pure" cases, meaning I considered the strain amplitude characteristic of each season as fixed throughout the entire lifespan. **This allowed me to determine the settlement ranges of asphalt stiffness depending on seasonal temperature fluctuations, as shown in Figure 3.21.**

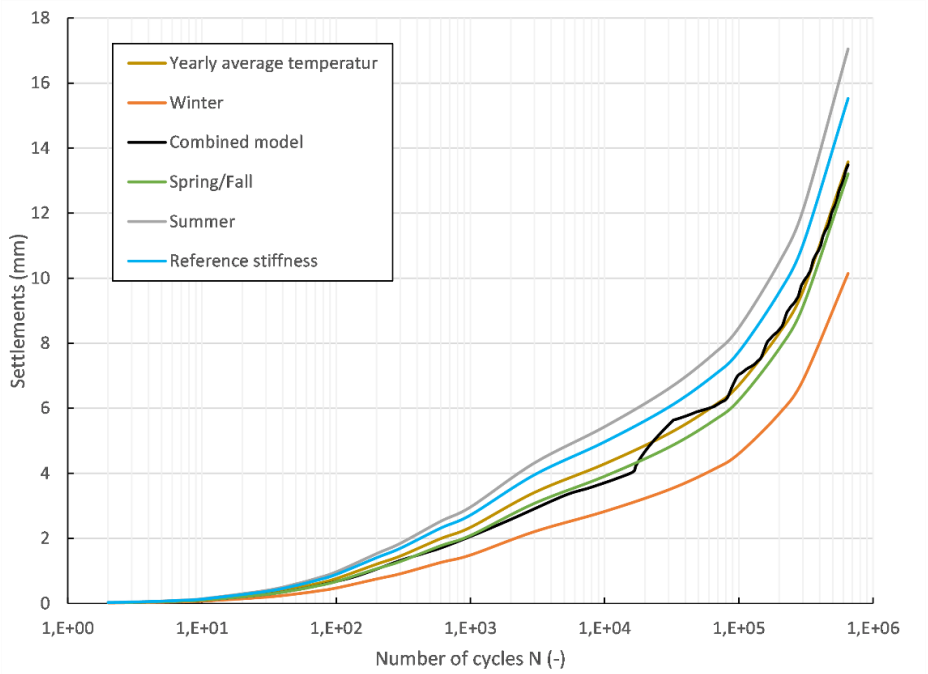

3.21. Figure: Calculated settlements on the surface of the base course in different seasons

I demonstrated through calculations that the settlements resulting from a fixed strain amplitude, based on the annual average temperature's corresponding asphalt stiffness, are of the same magnitude as those calculated by considering the deformation amplitudes for the winter-spring-summer-autumn seasons as successive cycle packages.

The settlements calculated based on the reference asphalt stiffness values determined in laboratory settings, as found in the literature, are approximately 15% greater than those calculated based on the annual average temperature. **I recommended that when accurately determining settlements due to repeated traffic loads, it is advisable to consider asphalt stiffness based on the annual average temperature.**

I examined the impact of the sequence of cycle packages, specifically whether the timing of when the road is opened to traffic matters, and whether it makes a difference when the road experiences the higher stresses associated with the softer summer asphalt. In this study, I varied the sequence of cycle packages based on possible seasonal combinations and evaluated the results**. My calculations showed that the sequence of cycle packages only has a significant impact until the end of the first year. As the number of cycles increases, the initial differences disappear, and the curves converge. By the end of the lifespan, the difference is less than 2% (Figure 3.22):**

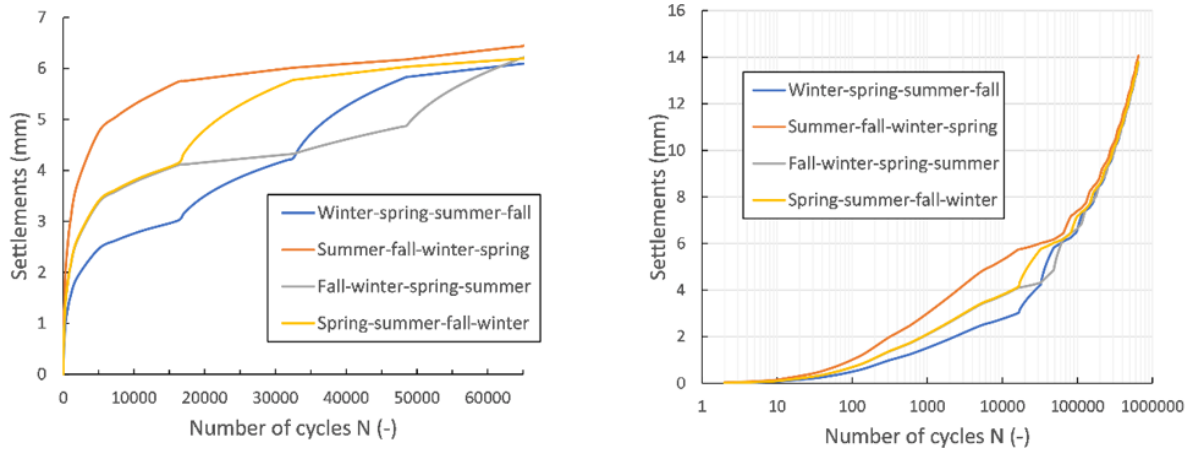

3.22. Figure: The effect of the order of cycle packages on the settlement: a) in the first year in a linear scale, b) over the entire design lifetime in a semi-logarithmic scale

4.4. New scientific result

I compared the load-bearing requirements of the standard pavement cross-sections specified in the Hungarian e-UT06.03.13 with those of international empirically-based design methods. In doing so, I found that there is no significant difference in load-bearing requirements for either the subgrade or the crushed stone base layer. I also compared the cross-section of the Hungarian e-UT06.03.13 traffic load class "D" with the German RstO category "III" for the same design traffic. I found that the German specification is much stricter regarding both the crushed stone base layer and the asphalt thickness.

My calculations showed that the settlements at the surface of the base course directly beneath the wheel axle, given identical subgrade properties and an equivalent traffic load of 2 million repetitions, are 1.96 times greater with the cross-section prescribed by the Hungarian e-UT06.03.13 "D" traffic load class than with the cross-section calculated according to the German RStO "III" category (Figure 3.23).

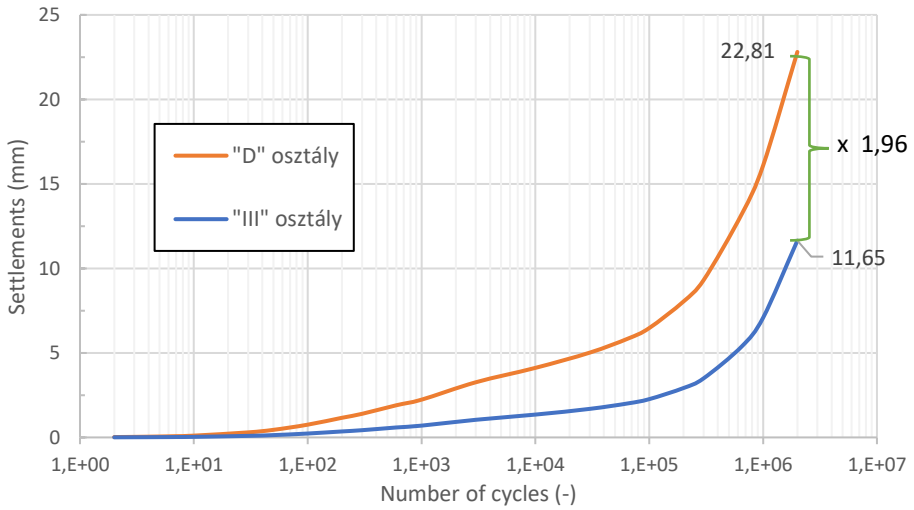

3.23. Figure: Settlements of the standard cross-sections of class „D" of hungarian e-UT06.03.13 in comparion of category „III" of RStO

Related publications: (Vámos and Szendefy, 2024b, 2024c, 2024d)

4 FUTURE RESEARCH POSSIBILITIES

The thesis presents a calculation method for determining soil-originated settlements in flexible pavement structures and provides a comprehensive overview of the main influencing factors. With the method presented, expected settlements on the top of the base layer can already be estimated during the design phase, allowing for appropriate measures to prevent limitations in the usability of the road structure. Hopefully, the findings of this dissertation will inspire research that leads to significant improvements in the quality of the national road network. Personally, I consider the most important outcome of this research to be the results related to the

thickness and material quality of the subbase layer, as these are the most effective in reducing potential settlements.

The determined settlements and settlement depression curves may initially seem somewhat exaggerated. This is due to certain simplifications made in the calculations to enhance safety, which I intend to refine in the future. The first factor to highlight is the role of temperature-dependent asphalt stiffness. During the research, I found that the reference asphalt stiffness measured in the laboratory does not align with the actual asphalt stiffness calculated based on the annual average temperature. As a result, the settlements presented in the thesis are approximately 15% greater than what might be expected under actual conditions. Secondly, it is important to note that in my calculations, I assumed a fixed axle spacing of 2.0 meters and that the wheel positions in the cross-section remain unchanged. In reality, vehicle axle spacings vary, and individual passes do not always occur along the symmetry axis of the lane. If we assume that individual vehicles pass with some variation around the centerline of the lane, the calculated maximum settlements would be smaller, while the settlements at points located at a distance of x from the wheel axle would be larger. Accordingly, the absolute settlements of the pavement structure and the relative settlement differences would show more realistic values.

In the calculations, I also assumed that the load was always identical to the standard axle load. In reality, however, vehicles in different vehicle classes have varying and typically smaller loads. I consider it advisable that in the future, calculations should account for the actual axle loads of vehicles participating in traffic, for example, based on statistical data.

The final settlements are influenced by the distribution of stress and deformation resulting from preloading. In my research, I used practical experience to determine the value of preloading during construction. I plan to conduct further research on the effects of different preloading values.

In my research, I did not examine the adverse effects arising from the wetting of the embankment. Since actual damage often results from inadequate drainage leading to wetting and the subsequent deterioration of stiffness, I consider it important to investigate this effect in the future.

Lastly, I would like to emphasize that the reliability of the results heavily depends on the input HCA parameters for the soils, which I determined solely through literature correlations. I consider it advisable to conduct laboratory tests on materials that conform to domestic road construction practices in the future, which would allow for more accurate estimation of the HCA parameters.

5 LIST OF PUBLICATIONS

5.1 Publications related to the new scientific results of the thesis

5.1.1 Foreign language journal article published abroad

Vámos, M.J., Szendefy, J., 2023a. Calculation Method for Traffic Load-Induced Permanent Deformation in Soils under Flexible Pavements. Geotechnics 2023, *3*(3), 955-974, https://doi.org/10.3390/geotechnics3030051

Vámos, M.J., Szendefy, J., 2024a. Determination of Permanent Deformations of Non-Cohesive Soils in Pavement Structures under Repeated Traffic Load. Eng 5, 1067–1084. https://doi.org/10.3390/eng5020058

Vámos, M.J., Szendefy, J., 2024b. On the Influencing Factors of Non-Asphalt Originated Rutting in Flexible Pavements. Transp. Infrastruct. Geotechnol. megjelenés alatt. https://doi.org/10.1007/s40515-024-00441-3

Vámos, M.J., Szendefy, J., 2024c. Temperature Effects on Traffic Load-Induced Accumulating Strains in Flexible Pavement Structures. Int. J. Pavement Res. Technol. megjelenés alatt. https://doi.org/10.1007/s42947-024-00466-4

5.1.2 Foreign language journal article published in Hungary

Vámos, M.J., Szendefy, J., 2023b. Overconsolidated Stress and Strain Condition of Pavement Layers as a Result of Preloading during Construction. Period. Polytech. Civ. Eng. 2023, 67(4), 1273-1283. https://doi.org/10.3311/PPci.22258

5.1.3 Hungarian-language journal article published in Hungary

Vámos M.J., Szendefy J., 2024d. Magyar és német típus-pályaszerkezetek várható süllyedéseinek összehasonlítása. ÚTÜGYI LAPOK, megjelenés alatt.

5.2 Other publications

Foreign language publication in the proceedings of an international conference

Vámos, M.J., Szendefy, J., 2014. Effect of pre-loading on dynamic soil properties and deformation characteristics, in: Proceedings of the 23rd European Young Geotechnical Engineering Conference. Barcelona, Spanyolország, pp. 11–14. Kiadó: ISSMGE London

Kissel, W., Vámos, M., Ramm, H. , Reul, O., 2020, Besondere Anforderungen an Setzungsprognose und Messverfahren am Beispiel des Teilchenbeschleunigers FAIR. in: Messen in der Geotechnik 2020, Heft 110, S. 59–85. Braunschweig: Institut für Grundbau und Bodenmechanik der TU Braunschweig

5.2.1 Hungarian-language journal article published in Hungary

Szendefy, J, Vámos M.J., 2014. A mésszel stabilizált talajok teherbírásának tartóssága, fagyállósága, Útügyi Lapok, 2 (3) 10p (2014)

Szendefy, J, Vámos M.J., 2014. Egyszerűsített és módosított Proctor-vizsgálati eredmények összehasonlítása I. Műszaki Ellenőr, 3 (11) pp 39-42 (2014)

Szendefy, J, Vámos M.J., 2014. Egyszerűsített és módosított Proctor-vizsgálati eredmények összehasonlítása II., Műszaki Ellenőr, 3 (11) pp 41-44 (2014)

5.2.2 Hungarian-language publication published in conference proceedings

Vámos, M.J., Szendefy, J., 2019. Laborvizsgálat homokok ciklikus alakváltozási tulajdonságainak meghatározásához, in: 5. Kézdi Konferencia Tanulmánykötete, pp 204-231, Budapest, Magyarország

Back, M.,Vámos, M.J., 2015. Telített és telítetlen lösz talajok dinamikus alakváltozási tulajdonságait befolyásoló tényezők, In: Köllő G (szerk.) XIX. Nemzetközi Építéstudományi Konferencia, pp 8-11, Csíksomlyó, Románia

Szendefy, J., Vámos, M.J., 2015. Újgenerációs hidraulikus kötőanyagkeverék laboratóriumi vizsgálati eredményeinek bemutatása, In: Köllő G (szerk.) XIX. Nemzetközi Építéstudományi Konferencia, pp 207-210, Csíksomlyó, Románia

Vámos, M.J., Szendefy, J., 2015. Modified Cam clay anyagmodell alkalmazása talajok ciklikus viselkedésének leírására, In: Köllő G (szerk.) XIX. Nemzetközi Építéstudományi Konferencia, pp 233-236, Csíksomlyó, Románia

Vámos, M.J., Szendefy, J., 2015. , In 4. Kézdi Árpád Emlékkonferencia Tanulmánykötete, pp238-248, Budapest, Magyarország

Szendefy, J., Vámos, M.J., 2014. Tömegstabilizáció első magyarországi tapasztalatai, In: Köllő G (szerk.) XVIII. Nemzetközi Építéstudományi Konferencia, pp 289-292, Csíksomlyó, Románia

Vámos, M.J., Szendefy, J., 2014. KÖVÉR AGYAGOK DINAMIKUS ALAKVÁLTOZÁSI TULAJDONSÁGAINAK MEGHATÁROZÁSA, In: Köllő G (szerk.) XVIII. Nemzetközi Építéstudományi Konferencia, pp 325-328, Csíksomlyó, Románia

Szendefy, J., Vámos, M.J., 2014. Újgenerációs kötőanyag az átmeneti talajok stabilizálásához, In: Geotechnika 2014 Konferencia, Paper 19, pp 15, Ráckeve, Magyarország

Vámos, M.J, Szendefy, J., 2014. Kövér agyagok dinamikus alakváltozási tulajdonságait befolyásoló tényezők, In: Geotechnika 2014 Konferencia, pp 1-15, Ráckeve, Magyarország

5.2.3 Editor of Conference Proceedings

Vámos, M.J, Szendefy, J. 2015. 4. Kézdi Árpád Emlékkonferencia Tanulmánykötete. Budapest: Budapesti Műszaki és Gazdaságtudományi Egyetem, Geotechnika és Mérnökgeológia Tanszék, 254 p. (2015)

5.2.4 Book (Educational)

Kovács, M, Szendefy, J., Vámos, M.J. 2014. Earthworks – Elektronic notes for the subject „Earthworks”. BME Geotechnika és Mérnökgeológia Tanszék, 2014

6 REFERENCES

AASHTO, 2002. AASHTO Guide for Design of Pavement Structures. American Association of State Highway and Transportation Officials.

Albayati, A.H., 2023. A review of rutting in asphalt concrete pavement. Open Eng. 13, 20220463. https://doi.org/10.1515/eng-2022-0463

Aljbouri, H.J., Albayati, A.H., 2023. Effect of nanomaterials on the durability of hot mix asphalt. Transp. Eng. 11, 100165. https://doi.org/10.1016/j.treng.2023.100165

Austroads, 2019. Guide to Pavement Technology Part 2: Pavement Structural Design.

Bharath, G., Kakade, V., Reddy, K.S., Tandon, V., Reddy, M.A., 2023. Investigation of rutting performance of dense and gap graded recycled asphalt mixtures. Innov. Infrastruct. Solut. 8, 252. https://doi.org/10.1007/s41062-023-01221-7

e-UT 06.03.13:2005, n.d. Aszfaltburkolatú útpályaszerkezetek méretezése és megerősítése, Útügyi Műszaki Előírás.

Gajári, G., 2019. A hengerelt aszfalt, mint részben telített, lehulés okozta izotróp sajátfeszültséggel bíró szemcsés anyag, viszko-hypoplasztikus anyagmodellje. Az Aszfalt XXVI. évfolyam, 58–72.

Gajári, G., Kisgyörgy, L., Ádány, S., Mahler, A., Lógó, J., 2021. A Visco-hypoplastic Constitutive Model for Rolled Asphalt. Period. Polytech. Civ. Eng. https://doi.org/10.3311/PPci.17515
KSH, 2024. Éves összefoglaló táblák (2023) a szállítás közlekedés témakörében 24.1.1. táblázatok.
Magyar Közút, N.Zrt., 2024. AZ ORSZÁGOS KÖZÚTHÁLÓZAT INFORMÁCIÓS EREDMÉNYTÁBLÁI 2023.
Morris, J., 1973. The prediction of permanent deformation in asphalt concrete pavements. USA Transp. Group.
Niemunis, A., 2003. Extended hypoplastic models for soils (habilitáció). INSTITUTES FÜR GRUNDBAU UND BODENMECHANIK DER RUHR-UNIVERSITÄT BOCHUM, Bochum.
Niemunis, A., Wichtmann, T., Triantafyllidis, Th., 2005. A high-cycle accumulation model for sand. Comput. Geotech. 32, 245–263. https://doi.org/10.1016/j.compgeo.2005.03.002
Primusz, P., Tóth, Cs., 2009. A behajlási teknő geometriája. Közlekép. Szle. 2009/12, 18–24.
Qi, H., Zhang, X., Liu, J., Zhang, T., Lv, G., Cui, L., Xie, Q., 2022. Study on Deformation Characteristics of Low-Highway Subgrade under Traffic Load. Appl. Sci. 12, 3406. https://doi.org/10.3390/app12073406
RDO -Asphalt 09, 2009. Richtlinien für die rechnerische Dimensionierung des Oberbaus von Verkehrsflächen mit Asphaltdeckschicht.
Singh, A.K., Sahoo, J.P., 2021. Rutting prediction models for flexible pavement structures: A review of historical and recent developments. J. Traffic Transp. Eng. Engl. Ed. 8, 315–338. https://doi.org/10.1016/j.jtte.2021.04.003
Toth, C., Petho, L., Rosta, S., 2024. Performance Characterisation of High RA Asphalt Mixes – A Laboratory and Field Study. Balt. J. Road Bridge Eng. 19, 71–87. https://doi.org/10.7250/bjrbe.2024-19.628
Tóth, C., Primusz, P., 2020. New Hungarian Mechanistic-Empirical Design Procedure for Asphalt Pavements. Balt. J. Road Bridge Eng. 15, 161–186. https://doi.org/10.7250/bjrbe.2020-15.466
Uzan, J., 2004. Permanent Deformation in Flexible Pavements. J. Transp. Eng. 130, 6–13. https://doi.org/10.1061/(ASCE)0733-947X(2004)130:1(6)
Vámos, M.J., Szendefy, J., 2024a. Determination of Permanent Deformations of Non-Cohesive Soils in Pavement Structures under Repeated Traffic Load. Eng 5, 1067–1084. https://doi.org/10.3390/eng5020058
Vámos, M.J., Szendefy, J., 2024b. On the Influencing Factors of Non-Asphalt Originated Rutting in Flexible Pavements. Transp. Infrastruct. Geotechnol. megjelenés alatt. https://doi.org/10.1007/s40515-024-00441-3
Vámos, M.J., Szendefy, J., 2024c. Temperature Effects on Traffic Load-Induced Accumulating Strains in Flexible Pavement Structures. Int. J. Pavement Res. Technol. megjelenés alatt. https://doi.org/10.1007/s42947-024-00466-4
Vámos, M.J., Szendefy, J., 2023a. Calculation Method for Traffic Load-Induced Permanent Deformation in Soils under Flexible Pavements. Geotechnics.
Vámos, M.J., Szendefy, J., 2023b. Overconsolidated Stress and Strain Condition of Pavement Layers as a Result of Preloading during Construction. Period. Polytech. Civ. Eng. https://doi.org/10.3311/PPci.22258
Vámos M.J., Szendefy J., 2024d. Magyar és német típus-pályaszerkezetek várható süllyedéseinek összehasonlítása. ÚTÜGYI LAPOK megjelenés alatt.
Verstraeten, J., Veverka, V., Francken, L., 1982. Rational and Practical Designs of Asphalt Pavements to Avoid Cracking and Rutting., in: Proceedings Fifth International Conference on Structural Design of Asphalt Pavements, 5. Delft University of Technology, pp. 45–58.
Werkmeister, S., 2003. Permanent Deformation Behaviour of Unbound Granular Materials in Pavement Constructions (Ph.D. értekezés). TU Dresden, Drezda.
White, T.D., Haddock, J.E., Hand, A.J.T., Fang, H., 2002. Contributions of Pavement Structural Layers to Rutting of Hot Mix Asphalt Pavements, NCHRP Report 468. National Academy Press, Washington D.C.
Wichtmann, T., 2016. Soil behaviour under cyclic loading - experimental observations, constitutive description and applications (habilitáció).
Wichtmann, T., 2005. Explicit Accumulation Model for Non-cohesive Soils under Cyclic Loading, Schriftenreihe des Institutes für Bodenmechanik der Ruhr-Universität Bochum. Bochum.
Wichtmann, T., Niemunis, A., Triantafyllidis, T., 2015. Improved simplified calibration procedure for a high-cycle accumulation model. Soil Dyn. Earthq. Eng. 70, 118–132. https://doi.org/10.1016/j.soildyn.2014.12.011
Wichtmann, T., Niemunis, A., Triantafyllidis, T., 2014. Flow rule in a high-cycle accumulation model backed by cyclic test data of 22 sands. Acta Geotech. 9, 695–709. https://doi.org/10.1007/s11440-014-0302-7
Wichtmann, T., Rondón, H., Niemunis, A., Triantafyllidis, T., Lizcano, A., 2010. Prediction of Permanent Deformations in Pavements Using a High-Cycle Accumulation Model. J. Geotech. Geoenvironmental Eng. 136. https://doi.org/10.1061/(ASCE)GT.1943-5606.0000275
Wichtmann, T., Triantafyllidis, T., 2015. Inspection of a high-cycle accumulation model for large numbers of cycles (N=2 million). Soil Dyn. Earthq. Eng. 75, 199–210. https://doi.org/10.1016/j.soildyn.2015.04.008
Wichtmann, T., Triantafyllidis, T., 2013. Effect of Uniformity Coefficient on G/Gmax and Damping Ratio of Uniform to Well-Graded Quartz Sands. J. Geotech. Geoenvironmental Eng. 139, 59–72. https://doi.org/10.1061/(ASCE)GT.1943-5606.0000735

Wichtmann, T., Triantafyllidis, T., 2010. On the influence of the grain size distribution curve on P-wave velocity, constrained elastic modulus Mmax and Poisson's ratio of quartz sands. Soil Dyn. Earthq. Eng. 30, 757–766. https://doi.org/10.1016/j.soildyn.2010.03.006

Zeißler, A., 2021. Grundlagen zur Struktur- und Materialoptimierung von Asphaltbefestigungen (habilitáció). TU Drezda, Drezda.

Zhang, J., Cao, J., Huang, W., Shi, X., Zhou, X., 2023. Rutting prediction and analysis of influence factors based on multivariate transfer entropy and graph neural networks. Neural Netw. 157, 26–38. https://doi.org/10.1016/j.neunet.2022.08.030

Zhou, P., Cui, L., Zhang, X., Ma, C., Liu, J., Shao, Y., Lv, G., Xie, Q., 2022. Study on Deformation Characteristics of Extended Highway in Operation Period. Adv. Civ. Eng. 2022, 1–13. https://doi.org/10.1155/2022/5496999